Ultrastructure of Kunjin Virus-Infected Cells: Colocalization of NS1 and NS3 with Double-Stranded RNA, and of NS2B with NS3, in Virus-Induced Membrane Structures

EDWIN G. WESTAWAY,[1]* JASON M. MACKENZIE,[1] MARK T. KENNEY,[1]
MALCOLM K. JONES,[2] AND ALEXANDER A. KHROMYKH[1]

*Sir Albert Sakzewski Virus Research Centre, Royal Children's Hospital, Brisbane 4029,[1] and Centre for
Microscopy and Microanalysis, University of Queensland, Brisbane 4072,[2] Australia*

The subcellular location of the nonstructural proteins NS1, NS2B, and NS3 in Vero cells infected with the flavivirus Kunjin was investigated using indirect immunofluorescence and cryoimmunoelectron microscopy with monospecific antibodies. Comparisons were also made by dual immunolabelling using antibodies to double-stranded RNA (dsRNA), the putative template in the flavivirus replication complex. At 8 h postinfection, the immunofluorescent patterns showed NS1, NS2B, NS3, and dsRNA located in a perinuclear rim with extensions into the peripheral cytoplasm. By 16 h, at the end of the latent period, all patterns had changed to some discrete perinuclear foci associated with a thick cytoplasmic reticulum. By 24 h, this localization in perinuclear foci was more apparent and some foci were dual labelled with antibodies to dsRNA. In immunogold-labelled cryosections of infected cells at 24 h, all antibodies were associated with clusters of induced membrane structures in the perinuclear region. Two important and novel observations were made. First, one set of induced membranes comprised vesicle packets of smooth membranes dual labelled with anti-dsRNA and anti-NS1 or anti-NS3 antibodies. Second, adjacent masses of paracrystalline arrays or of convoluted smooth membranes, which appeared to be structurally related, were strongly labelled only with anti-NS2B and anti-NS3 antibodies. Paired membranes similar in appearance to the rough endoplasmic reticulum were also labelled, but less strongly, with antibodies to the three nonstructural proteins. Other paired membranes adjacent to the structures discussed above enclosed accumulated virus particles but were not labelled with any of the four antibodies. The collection of induced membranes may represent virus factories in which translation, RNA synthesis, and virus assembly occur.

The ultrastructure of flavivirus-infected cells has often been described and includes several unique membranous structures induced after infection (13, 32, 41). No direct association of a nonstructural (ns) protein(s) with any of these earlier described membranes has been reported, but NS1 was recently shown to be located in another induced membrane structure in dengue virus type 2 (DEN-2)-infected cells (35). Expression of the *Flavivirus* genome involves translation from one long open reading frame of 10 proteins, including seven ns proteins, in the gene order C-prM-E-NS1-NS2A-NS2B-NS3-NS4A-NS4B-NS5 (17, 46). These products are cleaved from the polyprotein by cell signal peptidases or a virus-specified protease and were all precisely defined first for Kunjin virus (KUN) in regard to their termini and amino acid sequence (17, 47–49). Viral RNA is replicated in cells by a flavivirus-specified RNA-dependent RNA polymerase (RDRP), but the composition and structure of the RDRP complex have received relatively little attention. The flavivirus-specified protease activity for cleavages in the cytosol at dibasic sites in the polyprotein was shown to require NS3 and NS2B (11). NS3 contains motifs characteristic for serine proteases in the amino-terminal region and for helicases in the carboxy-terminal region (11, 56). Similarly, NS5 contains motifs for methyl transferase and for RDRP (11, 30).

Although the expectations based on hydrophobicity profiles of the flavivirus polyproteins and the translation strategy are that NS3 and NS5 should be associated with the cytosol rather than being bound to membranes (17, 46), all the KUN gene products cosedimented with fast-sedimenting or "heavy" membranes, well separated from soluble cell proteins (15, 16). Proliferation of cell membranes induced during flavivirus infection was detected by electron microscopy in the perinuclear region, commencing at 8 to 9 h postinfection (41). Electron microscopy of the heavy membranes with accompanying RDRP activity (15, 16) showed that they included all the described membranes induced by KUN. Indirect immunofluorescence (IF) with antibodies to NS1 showed localization mainly in the perinuclear or juxtanuclear region and some pale reticular staining in cells infected with KUN (43, 58), DEN-2 (40), or yellow fever virus (7, 23). In IF with other antibodies, DEN-2 NS3 (40) and Japanese encephalitis virus NS3 and NS5 (18) were localized mainly in the perinuclear region of infected cells. Electron microscopy using immunogold labelling with antibodies to NS1 and NS3 in thin sections of DEN-2-infected cells revealed only diffuse or generalized labelling in the cytoplasm (40). Strong nuclear immunofluorescent staining by antibodies to NS5 was observed in yellow fever virus- and DEN-2-infected cells, in addition to diffuse cytoplasmic staining (7, 27). We showed recently by IF and immunoelectron microscopy that NS4B translocated to the nucleus of KUN-infected Vero cells (59). The subcellular localization of the remaining three small hydrophobic proteins NS2A, NS2B, and NS4A has not been explored by immunolabelling. It has thus not been possible to obtain an overview of the distribution of all the ns proteins in flavivirus-infected cells, and there is also a lack of consistency among the various reports.

In earlier studies IF analysis of KUN-infected Vero cells

* Corresponding author. Mailing address: Sir Albert Sakzewski Virus Research Centre, Royal Children's Hospital, Herston Rd., Brisbane 4029, Australia. Phone: (617) 3253 1400. Fax: (617) 3253 1401.

revealed that double-stranded RNA (dsRNA) extended from the perinuclear region in a faint network characterized by many small densely staining foci (42). According to our model of flavivirus RNA replication, dsRNA or replicative-form (RF) RNA appears to function as a recycling template for the replicative intermediate (RI) on which flavivirus RNA is synthesized asymmetrically in a semiconservative manner (13); antibodies to dsRNA inhibited KUN RNA synthesis in an in vitro RDRP assay (14). Confirmation of flavivirus RF as template was obtained by Bartholomeusz and Wright (3) in RDRP assays with KUN and DEN-2, and the conversion of RF to RI was blocked by antibodies to NS3 and NS5. Antibodies to Japanese encephalitis virus NS3 or NS5 decreased the in vitro synthesis of viral RNA (18). RF, RI, and genome-sized RNA sedimented with induced membranes and the active KUN replicative complex, but after detergent treatment to remove all membranes, the ns proteins NS3, NS2A, NS2B/NS4A, and possibly NS1 still remained with the active complex during an additional sedimentation cycle (15). Similar results for the ns protein composition of partially purified West Nile virus RDRP were obtained after its sedimentation from a cytoplasmic extract through a 20% glycerol cushion (24). Cryoimmunoelectron microscopy revealed that localization of DEN-2 NS1 in cytoplasmic vacuoles and newly described "vesicle packets" (VP) was accompanied by colocalization of dsRNA, which was supported by dual IF (35).

In order to extend our studies on the role of ns proteins in flavivirus replication, we have expressed NS1, NS2B, and NS3 of KUN from recombinant baculoviruses in insect cells (28, 29) for preparation of rabbit monospecific antiserum to each of the purified products. In the present study, we have used these antisera and other antibody preparations to compare by IF and by cryoimmunoelectron microscopy the distribution in KUN-infected cells of NS1, NS2B, NS3, and the RF (as dsRNA) during and after the latent period of about 15 h (57). The results have some relevance to the composition and intracellular location of the replication complex for the *Flavivirus* genus and may be applicable to other members of the *Flaviviridae*, including the hepatitis C virus and pestiviruses which all share essentially the same gene order and putative replication strategy.

MATERIALS AND METHODS

Cells and virus. Vero cells were grown and maintained after infection with KUN as described previously (57).

Antibodies. Rabbits were immunized with KUN NS1, NS2B, and NS3 proteins purified as follows. NS1 protein was expressed in *Spodoptera frugiperda* (Sf) cells using the baculovirus expression system and purified after electrophoresis of cell lysates from polyacrylamide gels by electroelution (29). Anti-NS1 antibodies were prepared by four subcutaneous immunizations with 50 to 100 μg of purified NS1 protein. NS2B and ΔNS3 (NS3 with the protease region deleted) were expressed as fusion proteins with glutathione-*S*-transferase (GST) in the baculovirus expression system and purified from Sf cell lysates using glutathione Sepharose beads (28). ΔNS3 protein was then released from the GST moiety by digestion with factor Xa protease. Full-length NS3 protein was expressed as a hexahistidine-NS3 fusion protein in the baculovirus expression system (28). Anti-NS3 antibodies were prepared by three subcutaneous immunizations with ~50 μg of purified ΔNS3 protein, followed by three subcutaneous immunizations with ~100 to 200 μg of partially purified His-NS3 protein (high-speed pellet from the lysate of cells infected with His-NS3 recombinant baculovirus and ~90% enriched in His-NS3 protein; data not shown). Anti-NS2B antibodies were prepared by five subcutaneous immunizations with ~50 μg of GST-NS2B fusion protein still attached to the beads, followed by intravenous immunization with ~50 μg of GST-NS2B fusion protein eluted off the beads with glutathione.

Mouse monoclonal antibodies specific for KUN NS1 were generously supplied by Roy Hall, Department of Microbiology, University of Queensland, Queensland, Australia (1). Guinea pig antibodies to synthetic dsRNA reactive with togavirus RNA replication complexes (33) were generously supplied by Jia-Yee Lee, Macfarlane Burnet Centre for Medical Research, Melbourne, Australia. Donkey antibodies specific for rabbit, guinea pig, or mouse immunoglobulin G (IgG), conjugated to fluorescein isothiocyanate (FITC) or to Texas red, and
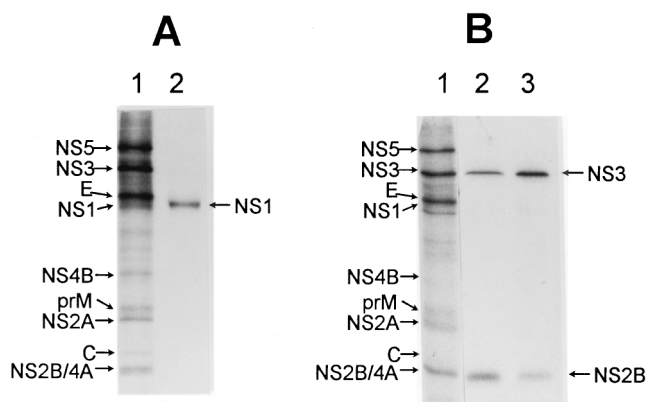
FIG. 1. Specificity of anti-NS1, anti-NS2B, and anti-NS3 rabbit antibodies prepared against purified KUN proteins (see Materials and Methods). (A) Capped RNA coding for NS1 protein was prepared as a runoff transcript from NS1 cDNA cloned into pBluescript II KS vector (Stratagene) and translated in a rabbit reticulocyte lysate (Promega) supplemented with canine microsomal membranes (Boehringer Mannheim) and [^{35}S]methionine/cysteine. The lysate was solubilized in radioimmunoprecipitation assay (RIPA) buffer (1% deoxycholate, 1% NP-40, 0.1% SDS, 0.1 M Tris-HCl [pH 7.5], 0.15 M NaCl) to release mature NS1 protein from the membranes and centrifuged at $15,000 \times g$ for 5 min to remove insoluble material, and a sample was radioimmunoprecipitated with anti-NS1 antibodies (lane 2) as described previously (59). (B) A $16,000 \times g$ cytoplasmic pellet from KUN-infected and metabolically labelled Vero cells prepared as described by Chu and Westaway (15) was solubilized in RIPA buffer, and samples were radioimmunoprecipitated as described in the legend to panel A with anti-NS2B (lane 2) or anti-NS3 (lane 3) antibodies. Lanes 1, marker lane in the 12.5% SDS-polyacrylamide gel which contains a sample of [^{35}S]methionine/cysteine-labelled cell lysate from KUN-infected cells. The calculated sizes of NS2B and NS3 are 14.4 and 68.9 kDa, respectively; NS1 is a glycoprotein with an estimated size of 44 kDa and migrates slightly ahead of E (see also Fig. 8).

mouse monoclonal antibodies to tubulin were purchased from Jackson Immunoresearch Labs.

Immunofluorescence. Cells on coverslips were infected at a multiplicity of infection of 2 to 10 and processed after fixation for IF as described previously (59); the standard fixation methods allowed penetration of antibodies into the cytoplasm only (using acetone at −20°C for 30 s) or permeabilized the nucleus for penetration by antibody (3.7% formaldehyde for 7 min followed by methanol for 10 min at 20°C). Dual-labelling experiments used FITC- and Texas red-conjugated species-specific anti-IgG. All photographs were taken using the oil immersion objective lens and were reproduced at the same magnification.

Cryofixation, cryosectioning, and immunogold-labelling of infected cells. Subconfluent cell monolayers were infected with KUN at a multiplicity of infection of 5. At 24 h postinfection, the cells were harvested and processed for cryosectioning and immunolabelling with protein A-gold (Batch 9608; Utrecht University), as described previously (59). For dual labelling, 50-nm sections labelled with the first antiserum and protein A-gold were quenched with 1% glutaraldehyde in phosphate-buffered saline and then immunolabelled with the second primary serum, using gold particles of a different size. Appropriate controls were prepared to ensure that there was no nonspecific binding of the antisera or cross-reactions with the gold-conjugated probes (35).

RESULTS

Specificity of rabbit antibodies to KUN NS1, NS2B, and NS3 and association of NS2B and NS3. Because of problems in resolving and identifying the small amounts of radiolabelled KUN NS1 in infected cell lysates (49, 57), the rabbit anti-NS1 antibodies were used to successfully immunoprecipitate in vitro-translated NS1 (Fig. 1A, lane 2). Using immunoblots, we confirmed the NS1 specificity and established lack of cross-reactivity with cell proteins; thus, the anti-NS1 antibodies reacted with purified NS1 prepared as for immunization (see Materials and Methods) but did not react with any Vero cell proteins (results not shown). Antibodies to NS2B precipitated radiolabelled NS2B and a smaller amount of NS3 from infected cell lysates under nondenaturing conditions (Fig. 1B, lane 2). Similarly, anti-NS3 precipitated NS3 and coprecipi-

tated a smaller amount of NS2B (Fig. 1B, lane 3). Coprecipitation of flavivirus NS2B and NS3 has been reported previously (2, 12). Anti-NS3 did not coprecipitate a truncated form, NS3′, as occurred with cell lysates of DEN-2-infected cells (2). Furthermore, all these antibodies were negative by IF (Fig. 2) and by immunogold labelling (see Fig. 5) in mock-infected cells.

Subcellular localization of NS1, NS2B, NS3, and dsRNA by IF. In view of our observation that KUN C and NS4B were translocated to the nucleus (59), we screened KUN-infected cells by IF with antisera to NS1, NS2B, and NS3 initially at 24 h, the time of maximum protein and RNA synthesis (13, 57), for cytoplasmic and nuclear localization, using the two standard methods of fixation (Materials and Methods). Similar patterns of distribution by IF were observed for all antibodies with either method. No nuclear staining was observed. Because of recent evidence that NS1 is associated with RNA replication (35, 37, 38) and because of the putative helicase activity of NS3 in replication and the known association of NS2B with NS3 in protease activity, we also used dual labelling at 24 h and earlier times postinfection with anti-dsRNA and antibodies to NS1, NS3, and NS2B.

NS1, NS2B, and NS3 were all strongly labelled by IF at 24 h postinfection in the perinuclear region, mainly showing irregularly shaped foci or inclusions, some of which extended outward into the cytoplasm in a coarse or punctate reticulum (Fig. 2A, panels 1, 3, and 5). Variation in the pattern and extent of staining varied from cell to cell; it was impossible to associate a specific pattern of staining with antibodies to any of the ns proteins. In a detailed analysis by IF of the distribution of NS1 in yellow fever virus-infected cells fixed in acetone, some variation in the staining pattern was also observed within the same culture or when using different monoclonal antibodies or different strains of virus (23). Perinuclear staining was thus observed either as multiple foci or as dense staining extending outward in the cytoplasm or alternatively as a pattern of fibrillar cytoplasmic staining. This last pattern was never seen with any of our KUN antibodies, but the two other patterns were observed in various proportions with all the antibodies to ns proteins, often in intermediate forms. We have not examined any other strains of KUN and hence are unable to comment on whether ns proteins of different strains localize in different sites. Staining by anti-dsRNA antibodies was confined to within the regions of subcellular localization of NS1, NS2B, and NS3, especially near the nucleus (Fig. 2A, compare panels 1 and 2, 3 and 4, and 5 and 6). Thus, although the staining patterns of the ns proteins were more widespread and variable than those for dsRNA, the extent of coincidence in staining was often striking, especially with anti-NS1 and with anti-NS3. The dsRNA foci were defined more sharply by FITC relative to Texas red staining and showed that the larger foci often comprised aggregates of small dots; there was also limited extension of dsRNA into reticular networks.

We next examined infected cells by IF during and at the end of the latent period. At 8 h postinfection, strong dual immunolabelling was obtained with anti-NS3 and anti-dsRNA (Fig. 2B, panels 1 and 2). IF with both antibodies was in a dense relatively thin perinuclear rim, possibly comprising aggregates of very small foci, and extended diffusely but not homoge-

neously outward throughout the rest of the cytoplasm. Similar but weaker staining at 8 h was produced also by anti-NS2B and mouse anti-NS1 antibodies, very similar in pattern to anti-dsRNA in dual-label IF (results not shown).

By 16 h postinfection NS1, NS2B, and NS3 were located by IF throughout the cytoplasm, mainly in fine reticular and punctate staining patterns densest in the perinuclear region, typical of endoplasmic reticulum (ER)-associated protein (Fig. 2A, panels 7, 9, and 11). At the same time, dual immunolabelling showed that dsRNA was now located mainly in discrete, somewhat irregular foci in the perinuclear region and beyond, against a background of relatively faint and diffuse nonhomogeneous staining (Fig. 2A, panels 8, 10, and 12). All major features of the dsRNA staining patterns existed within those of NS1, NS2B, and NS3 (Fig. 2A, compare panels 7 and 8, 9 and 10, and 11 and 12). Thus, dramatic changes had occurred between 8 and 16 h in the distribution of NS3 and dsRNA, which still overlapped but were becoming similar to the 24-h patterns. Similar changes appeared to be occurring in the subcellular localization of NS1 and NS2B, also in association with dsRNA.

Relationships by IF in subcellular distribution of NS1, NS3, and microtubules. It has been reported that at 30 h postinfection with KUN in Vero cells, close correlation by dual-label IF occurred in the filamentous staining produced by antitubulin antibodies and by antibodies to DEN-2 NS3 in cells treated with Triton X-100 (40). In untreated uninfected Vero cells the filamentous pattern produced by IF using antitubulin antibody (Fig. 3, panel 9) was clearly different from the dense perinuclear distribution of anti-NS3 antibodies in infected cells noted in Fig. 2A. Therefore, initial comparisons were made by dual-label IF of the subcellular distribution of NS3 and microtubules at 8 h postinfection, before the development of thickened perinuclear membranes (Fig. 2B, panel 1). Some coincidence may be present in the perinuclear region, but filaments like the microtubules could not be resolved elsewhere in the cytoplasm stained with anti-NS3 antibodies (Fig. 3, panels 1 and 2). Mild treatment at 20°C of infected cells with 0.01% Triton X-100 at 24 h partially dispersed the perinuclear accumulation of NS3, producing apparent partial coincidence with staining of microtubules (Fig. 3, panels 3 and 4). We achieved complete separation of antitubulin staining from NS3 by treatment of infected cells with 10 μg of vinblastine sulfate (Eli Lilly, Sydney, Australia) per ml from 8 to 24 h, followed immediately by cell fixation with acetone and dual IF staining with anti-NS3 and antitubulin. Vinblastine sulfate causes the disappearance of microtubules and formation of symmetrical microtubular bodies or crystals (4). Thus, after vinblastine treatment, the microtubules were dispersed and condensed into bacilliform rods in cytoplasm, as expected (4, 41, 42), but the treatment had no visible effect on the staining pattern of NS3 (Fig. 3, panels 5 and 6). Microtubules were disrupted also but did not condense after treatment of infected cells with 0.1% Triton X-100 at 20°C; when such cells were then fixed in acetone and dual labelled with anti-dsRNA and anti-NS3, prominent foci of dsRNA were still present, colocalized with some of the residual NS3, apparently still intact, and largely unaffected (data not

FIG. 2. (A) Comparable distribution by IF of ns proteins NS1, NS2B, and NS3 relative to dsRNA in KUN-infected Vero cells at 16 (panels 7 to 12) and 24 (panels 1 to 6) h postinfection. The KUN antisera to the ns proteins shown at the left of each row were prepared in rabbits, except for the mouse monoclonal antibody to NS1 in panel 7. (B) Comparable distribution of NS3 relative to dsRNA at 8 h (panels 1 and 2) and reactions of mock-infected cultures with each antibody as shown (panels 3 to 7). After IF labelling of the ns proteins in panels A and B with monospecific antibodies (using anti-rabbit or anti-mouse IgG conjugated to Texas red) at 8 and 24 h, the infected cultures were dual labelled using guinea pig anti-dsRNA and FITC-conjugated antibodies to guinea pig IgG. For the 16-h infected cultures, the labels were reversed. Cultures were either fixed at 24 h, using the formaldehyde-methanol method, or were fixed at 8 and 16 h with cold acetone.
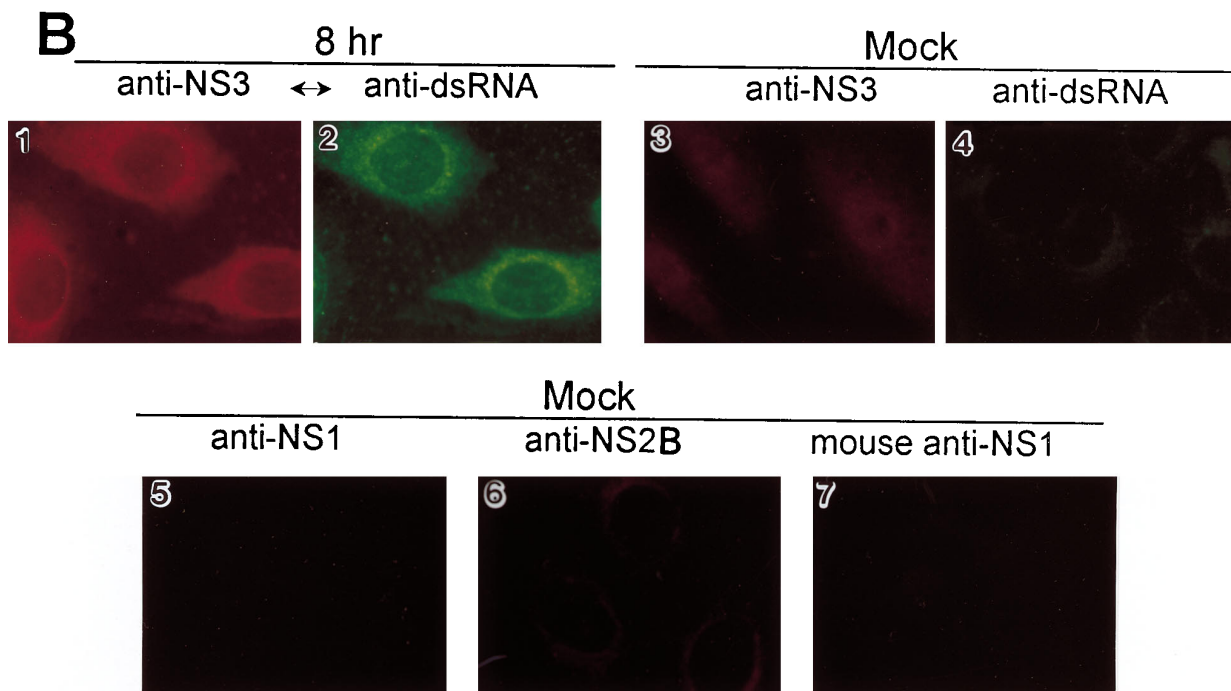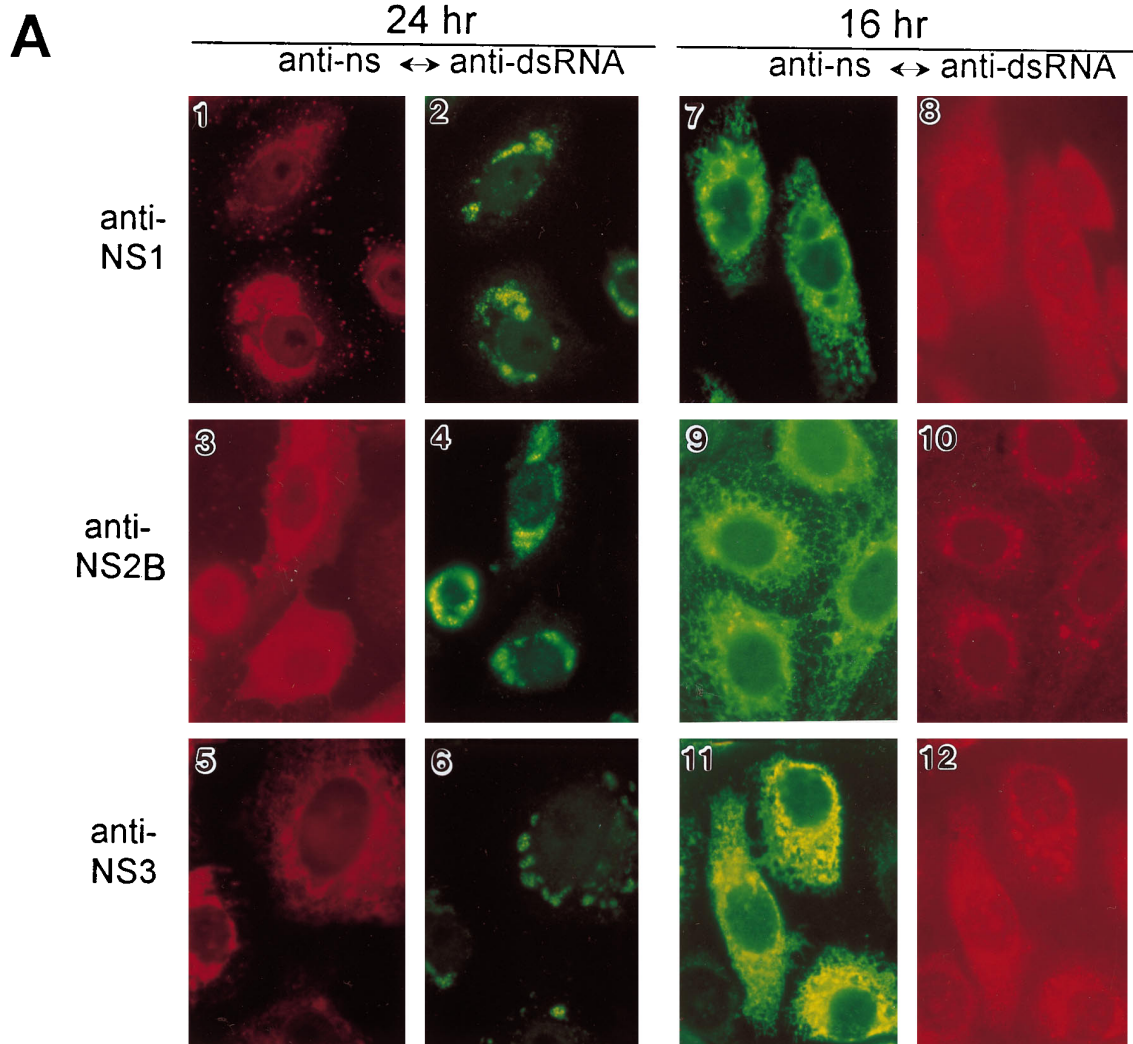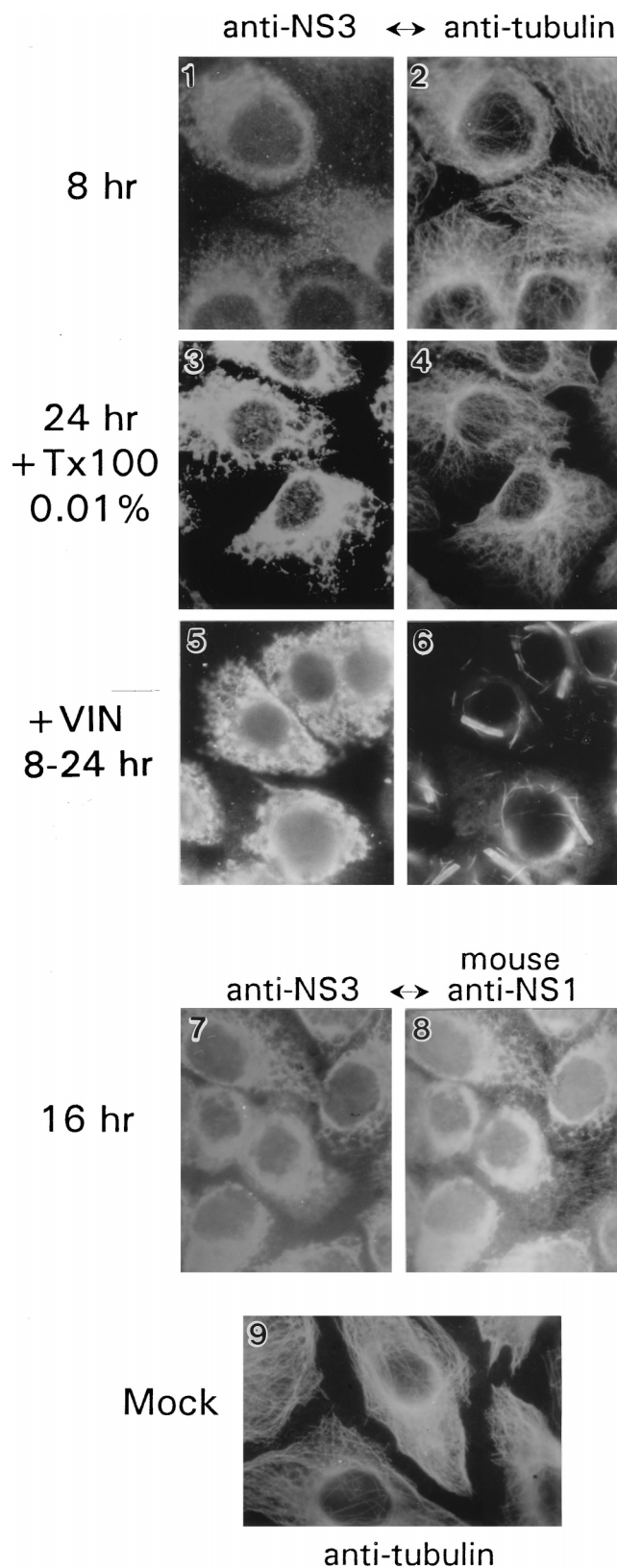
FIG. 3. Comparison by IF and dual immunolabelling with KUN-infected cells fixed in cold acetone of the subcellular locations of NS3 and microtubules at 8 h (untreated; panels 1 and 2), at 24 h after treatment with Triton X-100 (panels 3 and 4), and at 24 h after treatment for 16 h with vinblastine sulfate (VIN; panels 5 and 6) and of NS3 and NS1 at 16 h (untreated; panels 7 and 8).

shown), in accord with previous results of anti-dsRNA staining (41, 59).

Because the patterns of immunofluorescent staining obtained with anti-NS3 and anti-NS1 antibodies appeared similar at 16 h, before the complete development of thickened perinuclear membranes (Fig. 2, panels 7 and 11), we compared directly the subcellular localization of NS3 and NS1 at 16 h postinfection by dual labelling with rabbit and mouse antibodies, respectively. Excellent coincidence was noted (Fig. 3, panels 7 and 8). We concluded from this section that with the antibodies available, NS1 and NS3 were very closely associated by IF in cytoplasm and that NS3 had no apparent strong association with microtubules in KUN-infected Vero cells. Furthermore, the foci containing coincident dsRNA and NS3 were unaffected by treatment which disrupted microtubules. The distribution of microtubules appeared unchanged at least until 24 h postinfection.

Ultrastructural location of NS1, NS2B, and NS3 defined by immunoelectron microscopy. It has been known for many years that a proliferation of induced membranes occurs in flavivirus-infected cells. In thin sections of chemically fixed and resin-embedded cells, these induced membranes include convoluted membranes (CM), paracrystalline structures (PC), proliferating endoplasmic reticulum (ER), and vesicles of about 100 nm in diameter described as small, spherical smooth membrane structures (SMS) (15, 16, 32, 41). No specific function or role in flavivirus replication has ever been positively assigned to the CM, PC, or SMS. We decided to explore the ultrastructure of KUN-infected cells by immunogold labelling with our suite of antibodies used in IF (as described in the legend to Fig. 2). Cryosections were chosen because we wished to preserve the natural state of induced membranes and because antigenic sites in the sections are readily available for immunolabelling. For purposes of comparison, we first prepared both epon-embedded sections and cryosections at 24 h when virus-induced membranes were best defined by IF. In both types of section, we identified virus particles and the distinctive ultrastructure of CM, PC, and ER membranes (Fig. 4 and 5A). However, the SMS were visible only in the resin-embedded section, adjacent to the other induced membranes. Although not apparent in Fig. 4 and 5A, the virus-induced membranes were generally in the perinuclear region (compare with the IF patterns in Fig. 2).

Close inspection of the cryosection in Fig. 5A showed that the membranous structures were partially surrounded by virions, many in aggregates enclosed within smooth membranes continuous with paired membranes of the ER. Some of the latter may be rough ER, although ribosomes were often not clearly defined in the cryosections. Also evident in Fig. 5, but absent in Fig. 4, were the membranous structures recently described in DEN-2-infected cells as VP (35, 36). As in DEN-2-infected cells, the VP were immunolabelled by the anti-NS1 antibodies. Some gold particles were also associated with paired membranes of the ER leading into the CM, but none were within the PC and CM. PC and CM were generally found to be closely associated, and it has been reported that the PC appear to dissociate into CM late in KUN infection of Vero cells (41). In cryosections, intermediate forms of PC and CM were commonly observed in this study and PC were present as early as 16 h (see Fig. 7B). No virus particles and no CM, PC,

In panel 9, mock-infected cells were reacted with the mouse monoclonal antibodies to the tubulin used in panels 2, 4, and 6. Cells in panels 1, 3, 5, and 7 were immunostained with Texas red, the remainder with FITC.
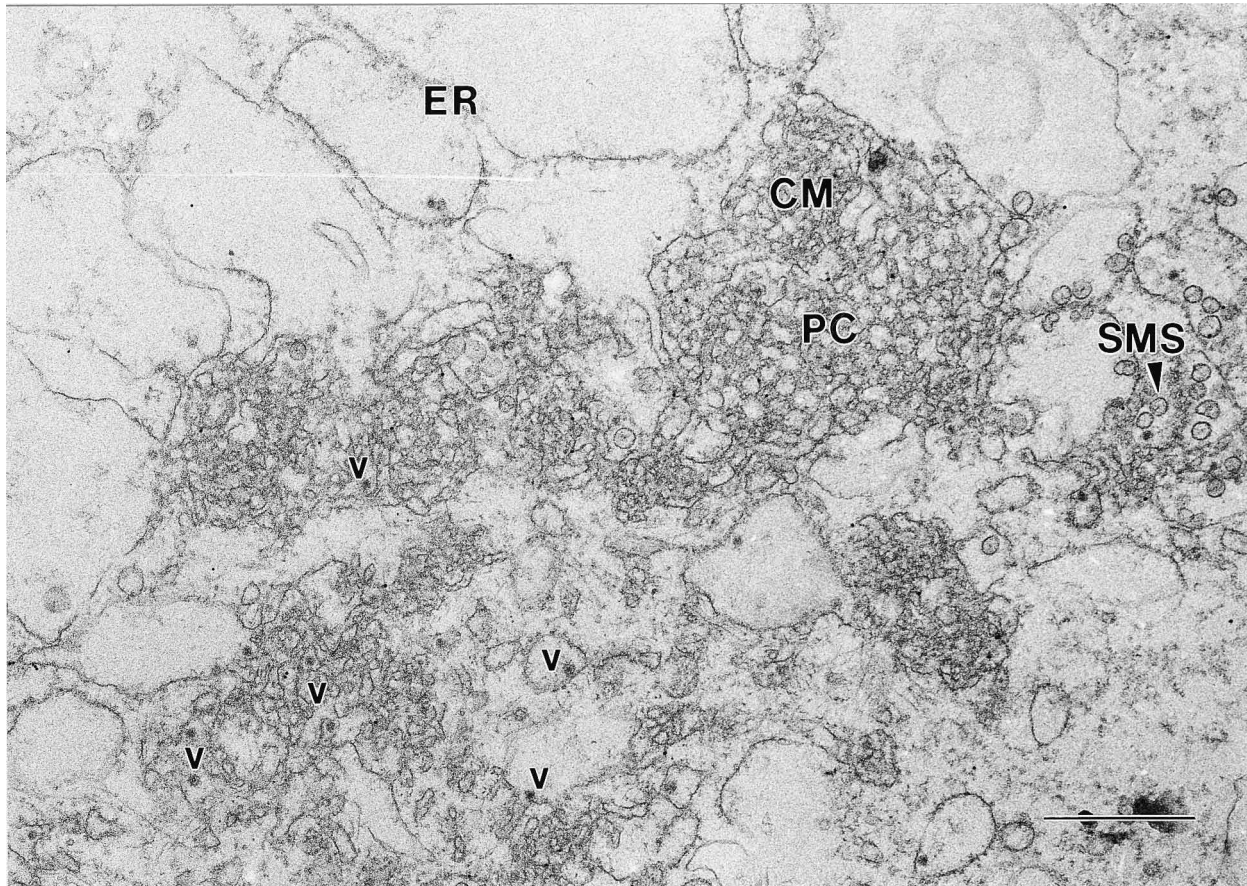
FIG. 4. Ultrathin section of chemically fixed and resin-embedded Vero cells at 24 h postinfection with KUN. Cells were embedded in Epon resin after fixation with 3% glutaraldehyde and staining with 2% uranyl acetate–lead citrate (35). Virus-induced structures include masses of CM, PC, and spherical SMS about 100 nm in diameter. Virus particles (v) and proliferating ER are in close proximity to the induced membranes. Bar, 500 nm.

or VP membrane structures were seen in mock-infected cells, which were not immunolabelled with any of the four polyclonal antibodies under study (Fig. 5B to E).

When cryosections were immunolabelled with either anti-NS2B or anti-NS3, PC arrays and CM were strikingly decorated with both antibodies (Fig. 6A to D). Gold particles were almost invariably superimposed on defined membranes, particularly evident in the CM, whereas the clear areas within the PC structures were generally devoid of gold particles. Membranes of the ER adjacent to the CM (Fig. 6B) or the nucleus (Fig. 6D) were immunolabelled with anti-NS2B and anti-NS3, respectively. Apart from one or two possibly random gold particles, a VP in Fig. 6B (and in other cryosections) was devoid of immunolabelled NS2B. In dual-labelled sections, NS2B and NS3 were enriched in the PC and CM structures and closely associated with each other (Fig. 6E and F), indicative of a common function in these induced membranes.

Association of NS1 and NS3 with anti-dsRNA in VP. VP were described in cryosections of DEN-2-infected Vero cells at 30 to 48 h (35, 36). When we examined KUN-infected cells for the presence of VP, they were readily identified at 24 h (Fig. 7A) and as early as 16 h (Fig. 7B). The VP were adjacent to perinuclear CM or PC arrays and as was the case for DEN-2, were immunolabelled with anti-NS1 antibodies (Fig. 7A) and dual labelled with anti-NS1 and anti-dsRNA antibodies (Fig. 7B). In contrast, the adjacent CM and PC structures were almost devoid of immunogold labelling with either antibody.

Also adjacent to the CM in Fig. 7A, virions were abundant in the lumen of paired ER membranes, which appeared to expand to enclose increasing numbers of virus particles. Some of the paired ER membranes containing virions appeared to be continuous with membranes at the periphery of the CM. As in Fig. 5A, there appeared to be no enrichment of immunolabelled NS1 associated with the accumulated virus particles in Fig. 7A.

When infected cells were dual labelled with anti-NS3 and anti-dsRNA, CM were strongly labelled with anti-NS3 antibodies as noted previously, but dual labelling was observed only in the VP (Fig. 7C and D). Individual vesicles in the VP were packed tightly in irregular shapes, roughly spherical, with approximate diameters of 50 to 100 nm. Each vesicle was enclosed by a bilayer membrane similar to that usually enveloping the VP. The sizes of the packets varied from approximately 200 to 500 nm. Immunogold-labelled NS3 was distributed randomly within the CM and VP, although several linear arrays comprising three or four adjacent gold particles were present in both Fig. 7C and D. Labelling of NS3 in the VP appeared to be mainly on the surfaces of individual vesicles which contained amorphous material separated from the bounding membrane.

In summary, immunolabelling of cryosections established that PC/CM structures containing NS2B and NS3 were involved in virus replication, and that NS3 was also a component of the putative replication complex with NS1 and dsRNA in
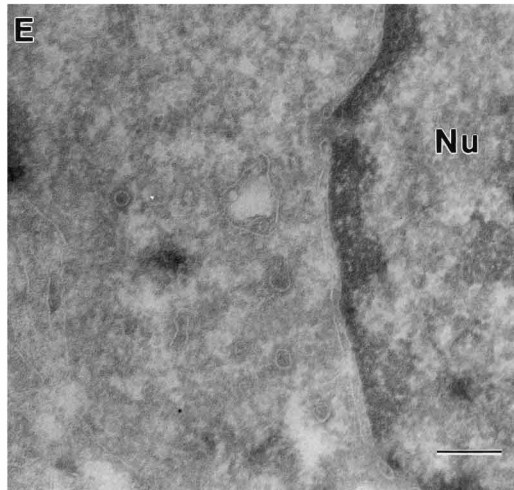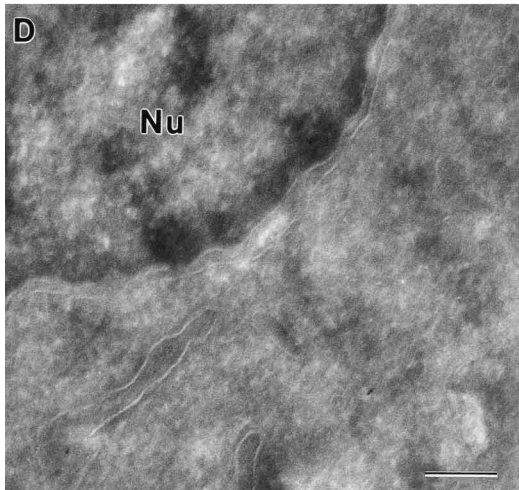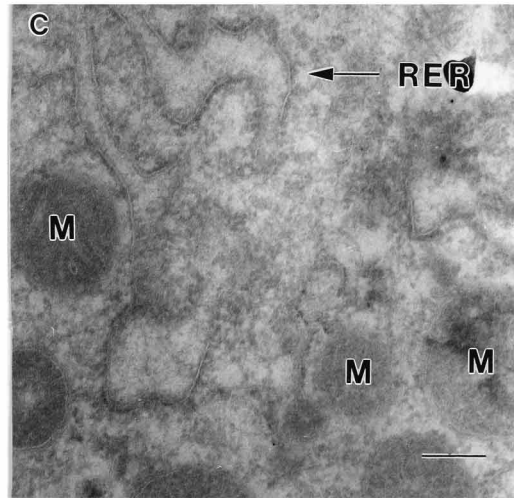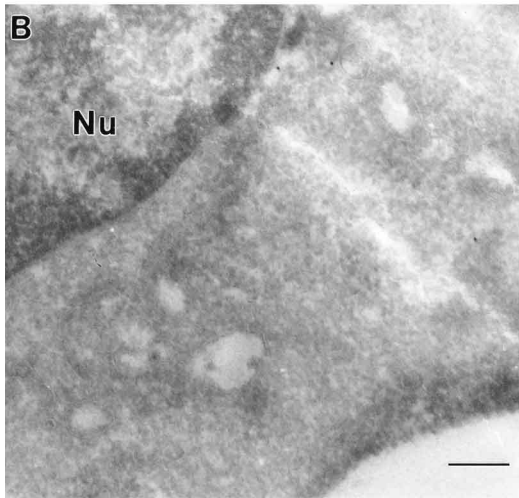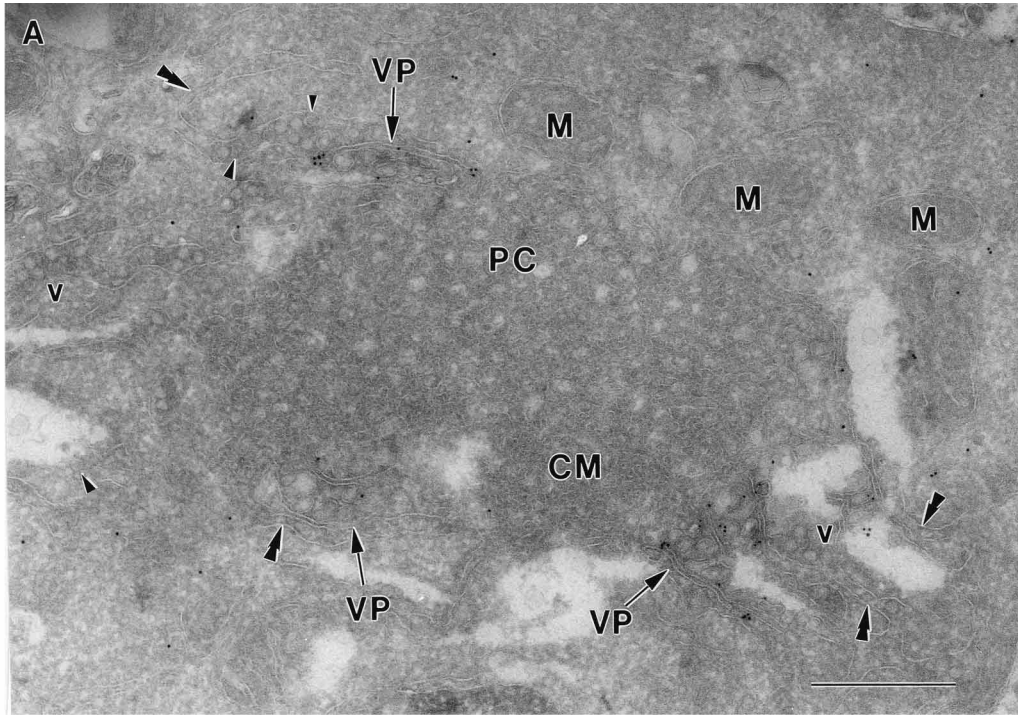
FIG. 5. Ultrathin cryosections of KUN-infected (A) or mock-infected (B to E) Vero cells. (A) Infected cells were harvested at 24 h, and sections were immunolabelled with anti-NS1 antibodies and 10-nm protein A-gold particles as described in Materials and Methods. Distinctive morphology is evident for virus-induced CM, PC, and VP apparently attached to the periphery of the PC/CM structures. Anti-NS1 antibodies consistently labelled the VP. In addition to these structures, collections of virions (v) are present in the vicinity of the CM and PC, and distinct cores (arrowheads) can be identified in some virus particles. Mock-infected cells were probed under the same conditions used for those in panel A as negative controls to confirm the viral specificity of anti-NS1 (B), anti-NS2B (C), anti-NS3 (D), and anti-dsRNA (E) antisera. Nu, nucleus; double arrowheads, ER; M, mitochondria. In panel C, the rough ER (RER) is prominent. Bars, 500 nm (A) and 200 nm (B to E).

VP. A close association of NS1, NS2B, and NS3 with induced membranes and with the ER was a common feature of analyses by IF and by immunoelectron microscopy.

Radiolabelled ns proteins in cell lysates associated with dsRNA by radioimmunoprecipitation. Confirmatory evidence of an association of a dsRNA template with ns proteins was sought by radioimmunoprecipitation of KUN-infected Vero cell lysates metabolically labelled with [^{35}S]methionine/cysteine. Thus, radiolabelled infected cell lysates were treated with 0.5% Nonidet P-40 (NP-40) for 30 min at 4°C, centrifuged to remove nuclei, and immunoprecipitated with anti-dsRNA. After sodium dodecyl sulfate (SDS)-gel electrophoresis, NS5, NS3, and a protein migrating identically with NS1 (below E in the E-NS1 doublet) were readily identified (Fig. 8, lanes 2 and 3). Additional virus-specific proteins in the immunoprecipitate were NS2B/NS4A (not resolved with certainty) and an apparently slightly truncated form of NS2A. The association of KUN ns proteins NS3, NS1, and possibly NS2B with dsRNA by immunoprecipitation was compatible with the IF data and immunogold labelling presented above. NS4B was only weakly radiolabelled in the original cell lysate when depleted of nuclei and was visible as a very faint band in the immunoprecipitate after a long exposure of the autoradiogram (data not shown). None of the structural proteins C, prM, and E present in the cytoplasmic extract could be detected in the immunoprecipitate (Fig. 8).

The results in this and previous sections are not only in accord with each other but also with our sedimentation analyses of membranes and of the purified active KUN RDRP complex in which radiolabelled NS3, NS2A, NS2B, and possibly NS1 appeared to remain associated with the detergent-treated complex (NS5 was degraded), whereas the structural proteins were absent from the complex (15).

DISCUSSION

These results provide the first direct evidence of an association of the CM/PC structures induced in flavivirus-infected cells with two ns proteins, namely NS2B and NS3. Protease activity has been established for NS3 in conjunction with cofactor NS2B, producing cytoplasmic cleavages in *cis* and sometimes in *trans* at the junctions NS2A-2B-3-4A and NS4B-5, at a site characterized generally by Lys/Arg-Lys/Arg ↓ Gly/Ser/Ala, but Gln occurs between the dibasic residues at the NS2B ↓ NS3 cleavage site of the dengue viruses (2, 8, 10, 20, 21, 34, 45). NS2B contains a central conserved hydrophilic region flanked by hydrophobic domains, and mutations or deletions within the conserved region abolished or dramatically reduced cleavage efficiency, abolished recovery of infectious virus, and affected an observed association between NS2B and the NS3 protease domain (12, 21). In contrast to NS2B, NS3 is predominantly hydrophilic (17) and was removed from stringently washed membranes of West Nile virus-infected cells, whereas NS2B was not solubilized (55). Our observation that NS2B and NS3 were closely colocalized by cryoimmunoelectron microscopy within the CM/PC structures appears to implicate these induced membranes for the first time directly in

the events of flavivirus replication. The absence of detectable NS1 (present results) and of NS4B (59) from the CM/PC structures is consistent with the notion that these membranes are the site of proteolytic cleavages of the nascent polyprotein by the NS2B-NS3 protease, in which the presence of other ns proteins is only transient and hence not easily detectable by immunoelectron microscopy. However, a necessary corollary is that the nascent polyprotein associated with the adjacent rough ER and/or polysomes could expose its dibasic cleavage sites within the CM/PC structures during translation.

A second major observation is the demonstrated close association of dsRNA with NS3 and NS1 by IF and more dramatically by cryoimmunoelectron microscopy within the membranes of the recently described VP (36). The physical association of NS1 and NS3 with membranes is relatively weak, both being released from stringently washed membranes of West Nile virus-infected cells (55). Like NS3, NS1 is predominantly hydrophilic but is cleaved at both termini within the lumen of the rough ER, rather than in the cytosol as occurs for NS3 (17). Thus, as expected, membrane-bound NS1 in cell lysates of DEN-2- or KUN-infected cells was protected from digestion by trypsin, whereas NS3 was not protected by membranes (9). NS1 contains no apparent motifs associated with replication, but DEN-2 NS1 has been implicated in RNA synthesis by subcellular colocalization in VP with anti-dsRNA (35) as shown here for KUN NS1. Furthermore, in experiments with yellow fever virus NS1, ablation of glycosylation sites, or charged-amino-acid-to-alanine mutagenesis, caused early delays in RNA synthesis and virus production or produced a temperature-sensitive (*ts*) mutant leaky at 39°C with similar but more severe inhibitory effects, respectively (37, 38). Although helicase activity has not been directly associated with flavivirus NS3, RNA-stimulated nucleoside triphosphatase activity was demonstrated with full-length and N-terminally truncated NS3 of West Nile, yellow fever, and Japanese encephalitis viruses (31, 50, 52–54). The demonstrated associations of NS1 and NS3 with dsRNA by immunogold labelling strongly implicate both ns proteins as components of a flavivirus replication complex (RC) located within the induced VP. NS3 may function as a helicase within the RC, and NS1 may interact with the RC by directing it to the membranes of VP, similarly to the demonstrated function of the poliovirus 2C protein (5) and as suggested by Mackenzie et al. (35).

Membranous masses similar to the PC arrays occur in other contexts. In some uninfected Vero cells, prolonged treatment (30 h) with vinblastine sulfate produced dense paracrystals with an appearance similar to that of the PC, apparently derived from disrupted microtubules (26). In other experiments (41), similar treatment of KUN-infected cells produced rodlike crystals viewed by IF after immunostaining with antitubulin and with cross-reacting antibodies to DEN-2 NS3. As noted in Results (see above and Fig. 3), we were unable to show colocalization of microtubules and NS3 using homologous antibodies at 8 h or after treatment with Triton X-100 or vinblastine sulfate at 24 h in KUN-infected cells under similar conditions to those used by Ng and Hong (41). Membranes strikingly similar to the flavivirus CM/PC were also induced in CHO cells
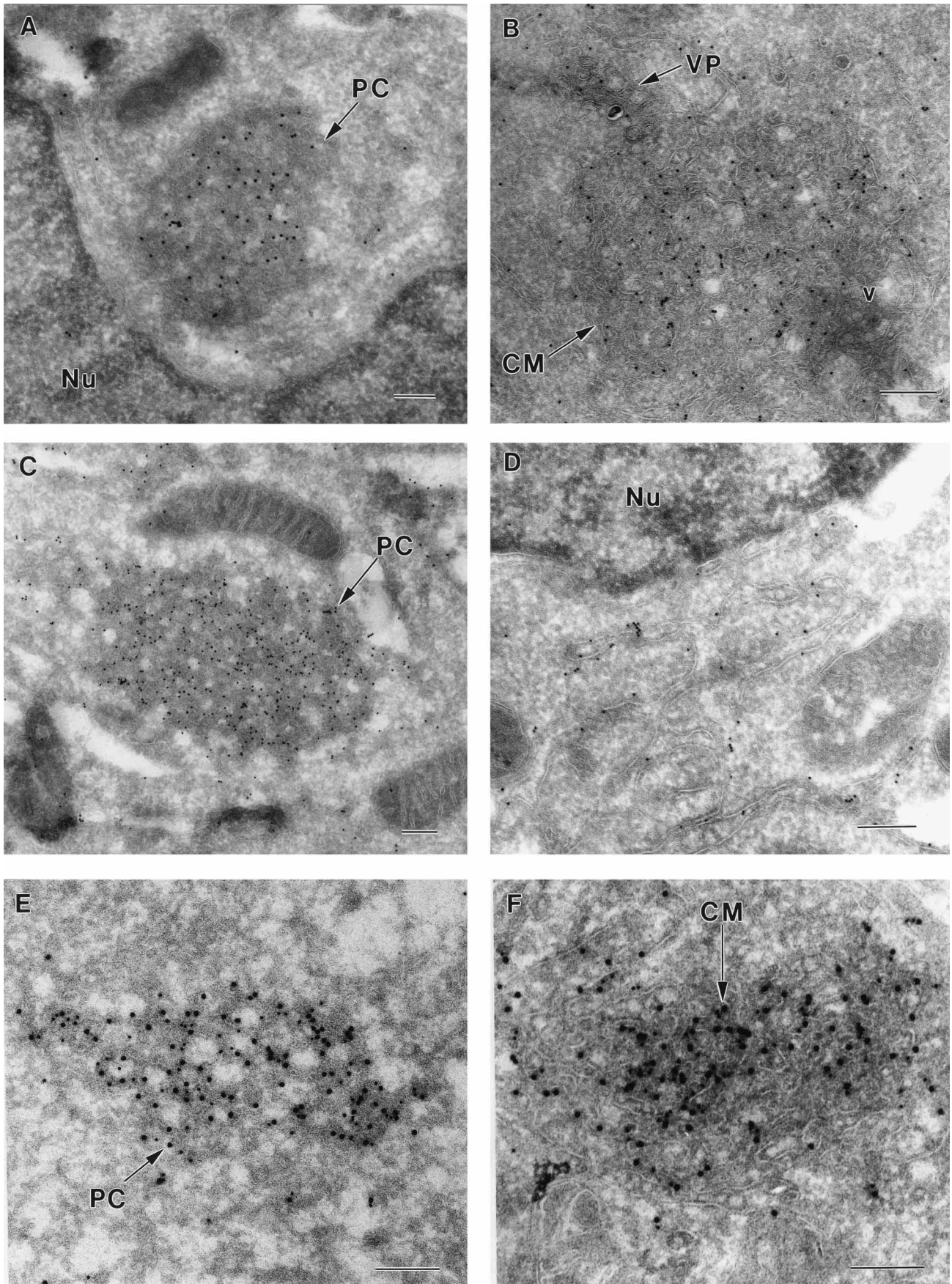
FIG. 6. Subcellular immunolocalization in cryosections of KUN-infected cells of NS2B and NS3. (A and B) Immunogold-labelled NS2B (10-nm particles) was strongly enriched in the PC and CM structures, respectively, but anti-NS2B did not appear to significantly label a VP (arrow). (C and D) Immunogold-labelled NS3 (10-nm particles) was strongly associated with a PC array and with membranes of the perinuclear ER, respectively. (E and F) Dual immunolabelling with NS2B (10-nm gold particles) and NS3 (15-nm particles) revealed their colocalization within the PC (E) and CM (F). Nu, nucleus. Bars, 200 nm.
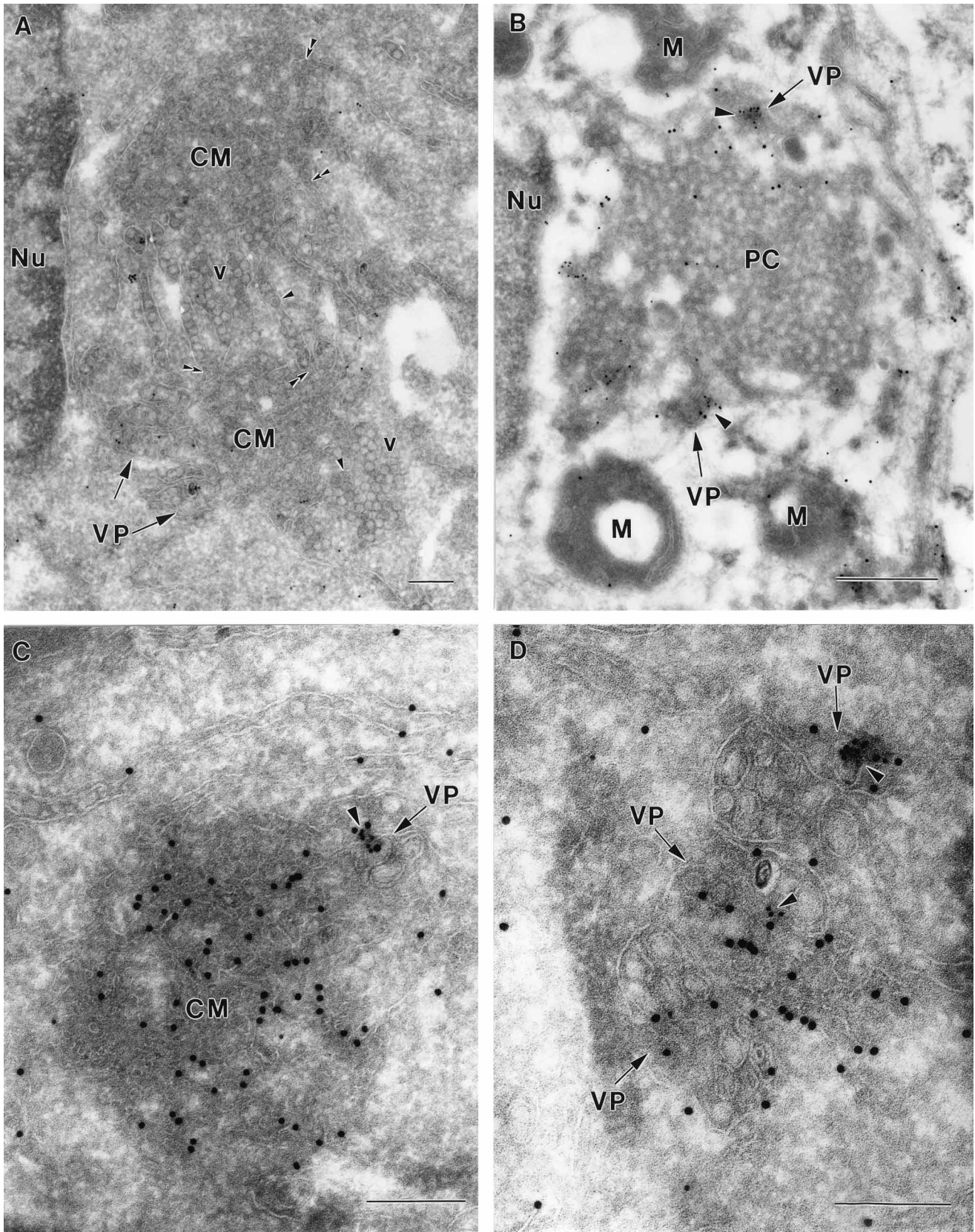
FIG. 7. Ultrathin cryosections of KUN-infected cells immunolabelled with anti-NS1, anti-NS3, and anti-dsRNA antibodies at 24 h, except for those in panel B (16 h). (A) Protein A-gold labelled (10 nm) anti-NS1 antibodies in several VP apparently attached to two regions of CM connected by paired membranes of the ER engorged in the lumen with virus particles (v), all in close proximity to the nucleus (Nu). Double arrowheads indicate regions of continuity between the ER and CM. (B) Dual labelling with anti-NS1 (15-nm gold particles) and anti-dsRNA (10-nm particles) enriched in densely stained VP on the periphery of a PC mass adjacent to the nucleus (Nu). (C and D) Immunogold-labelled NS3 (15-nm particles) and dsRNA (10-nm particles) were present in the VP in panels C and D, but NS3 only was enriched also in the CM in panel C. Arrowheads indicate cores visible within virus particles in panel A and regions of coincidence of dual immunogold labelling in panels B, C, and D. Bars, 200 nm (A, C, and D) and 500 nm (B).
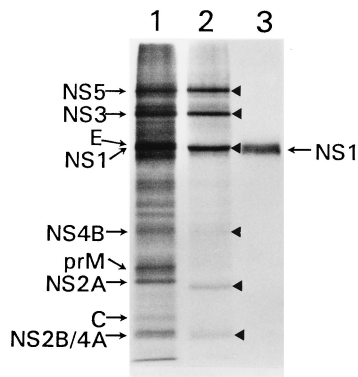
FIG. 8. Identification of KUN ns proteins immunoprecipitated from the cytoplasmic fraction of infected Vero cell lysates by anti-dsRNA antibodies. Infected cells were labelled from 24 to 30 h with [³⁵S]methionine/cysteine, and the nuclei were removed by low-speed centrifugation after treatment of cells with 0.5% NP-40. Aliquots of the cytoplasmic extract were electrophoresed in a 12.5% SDS-discontinuous gel before (lane 1) or after immunoprecipitation in RIPA buffer with anti-dsRNA antibodies and protein A-Sepharose beads (lane 2). In lane 3, labelled NS1 as marker (arrow) was prepared as described in the legend to Fig. 1A. The gel was dried prior to autoradiography. Arrows and arrowheads in lanes 1 and 2, respectively, indicate KUN-specific proteins identified in the cytoplasmic fraction and immunoprecipitate.

stably transformed using a plasmid expressing only the E1 envelope glycoprotein of rubella virus, and their juxtanuclear location was described as a novel post-ER pre-Golgi compartment lacking rough ER and Golgi membrane proteins (25). It would be premature to postulate a similar origin for the naturally occurring flavivirus-induced CM/PC structures.

The VP have a striking similarity in their ultrastructure to cryosections of special lysosomes which are multivesicular major histocompatibility complex (MHC) class II-containing compartments and act as peptide transporters in cells expressing MHC-II molecules (see especially Fig. 6B in reference 60). The vesicles within the packets comprising VP are similar in size to the SMS (Fig. 4) which appear as clusters enclosed within the ER adjacent to CM/PC masses in sections of chemically fixed cells infected with Japanese encephalitis, KUN, or West Nile viruses (15, 16, 32, 39, 41, 44). It is of interest that in togavirus-infected cells, so-called cytopathic vacuoles I (CPI) or replication complexes contain vesicles very similar in appearance to those of the flavivirus SMS but which line the inside of the CPI-bounding membrane (reference 22 and references therein; 33). Alphavirus CPI were identified as replication complexes by the presence of immuno-gold-labelled viral RNA polymerase on the cytoplasmic surface of CPI which were shown to be modified secondary lysosomes and endosomes (22), and rubella virus replication complexes were identified by immunogold labelling with antibodies to dsRNA (33). We are attempting to compare immunolabelling of VP and of SMS in KUN-infected cells to explore any relationship between them and the association of any ns proteins additional to NS1 and NS3 within the induced VP. Of particular interest is the threadlike structure enclosed within the SMS (15, 16, 32, 39, 41, 44) which appears to be represented by a dense core in cryosubstituted West Nile virus-infected Vero cells (44).

Viral plus-strand RNA synthesis is assumed to be initiated on the double-stranded RF of poliovirus (5) as for flaviviruses (13). Identification of VP in cryosections as the putative site of the flavivirus RC allows some comparison with the poliovirus RC which appears by negative staining to be enclosed within an induced rosettelike structure with peripheral smooth membrane vesicles 200 to 400 nm in diameter and originating from

the rough ER (5). In thin sections, immunogold labelling for template RNA is enriched over vesiculated areas of the poliovirus RC (51) or the flavivirus VP (Fig. 7) (35). In both cases, the viral RNA polymerase activity in cytoplasm occurs in two fractions of sucrose density gradients and persists after the associated membranes are dissolved by detergent (6, 15). The poliovirus RC remains active on individual vesicles dissociated at low temperature and low ionic strength (19). An essential difference is that genome-sized RNA was released from the detergent-treated but still active RC of KUN during further incubation but not from that of poliovirus. In infected cells, the flavivirus VP may provide an architectural framework for assembly of all the components of the RC and hence for a more rapid synthesis of progeny genomes.

During the initial stages of flavivirus replication, the induced membranes discussed above are obviously unavailable. The IF patterns of NS1, NS2B, and NS3 at 8, 16, and 24 h postinfection (Fig. 2) are in agreement with the report that the proliferation of induced membranes detected by electron microscopy of KUN-infected Vero cells does not commence until 8 to 9 h (41). The long induction period may account for the relatively long latent period of flaviviruses. Thus, KUN RNA synthesis and RNA polymerase activity were not detectable until after 8 h (13). Subsequently, PC and SMS develop and an interconversion of PC to CM appears to occur (41) in accord with the present results (Fig. 5). The proximity to each other of VP, CM/PC, and ER, in which virions often accumulate, and the immunolabelling results described herein suggest that sets of the flavivirus-induced membranes presently described comprise virus factories in which translation and proteolytic processing, RNA synthesis, and possibly virus assembly occur during the peak period of virus replication. A close association of the components of the proposed factories is indicated because in cells treated with Triton X-100, dual labelling by IF persisted for dsRNA with NS1 and NS3 (data not shown) and with NS4B and C with or without treatment (59). However, budding of virus particles was not observed in any of the cryosections. Identification of the origin of the flavivirus VP and CM/PC membranes requires analyses with membrane-specific markers and will be the subject of future studies, together with the location and roles in infected cells of NS2A, NS4A, and NS5.

ACKNOWLEDGMENTS

REFERENCES

1. **Adams, S. C., A. K. Broom, L. M. Sammels, A. C. Hartnett, M. J. Howard, R. J. Coelen, J. S. Mackenzie, and R. A. Hall.** 1995. Glycosylation and antigenic variation among Kunjin virus isolates. Virology **206:**49–56.
2. **Arias, C. F., C. F. Preugschat, and J. H. Strauss.** 1993. Dengue 2 virus NS2B and NS3 form a stable complex that can cleave NS3 within the helicase domain. Virology **193:**888–899.
3. **Bartholomeusz, A. I., and P. J. Wright.** 1993. Synthesis of dengue virus RNA in vitro: initiation and the involvement of proteins NS3 and NS5. Arch. Virol. **128:**111–121.
4. **Bensch, K. G., and S. E. Malawista.** 1969. Microtubular crystals in mammalian cells. J. Cell Biol. **40:**98–107.
5. **Bienz, K., D. Egger, M. Troxler, and L. Pasomontes.** 1990. Structural organization of poliovirus RNA replication is mediated by viral proteins of the P2 genomic region. J. Virol. **64:**1156–1163.
6. **Bienz, K., D. Egger, T. Pfister, and M. Troxler.** 1992. Structural and functional characterization of the poliovirus replication complex. J. Virol. **66:** 2740–2747.
7. **Buckley, A., S. Gaidamovich, A. Turchinskaya, and E. A. Gould.** 1992. Monoclonal antibodies identify the NS5 yellow fever virus non-structural protein in the nuclei of infected cells. J. Gen. Virol. **73:**1125–1130.
8. **Cahour, A., B. F. Falgout, and C.-J. Lai.** 1992. Cleavage of the dengue virus polyprotein at the NS3/NS4A and NS4B/NS5 junctions is mediated by viral protease NS2B-NS3, whereas NS4A/NS4B may be processed by a cellular protease. J. Virol. **66:**1535–1542.

9. **Cauchi, M. R., E. A. Henchal, and P. J. Wright.** 1991. The sensitivity of cell-associated dengue virus proteins and the detection of trypsin-resistant fragments of the nonstructural glycoprotein NS1. Virology **180:**659–667.

10. **Chambers, T. J., C. S. Hahn, R. Galler, and C. M. Rice.** 1990. Flavivirus genome organization, expression, and replication. Annu. Rev. Microbiol. **44:**649–688.

11. **Chambers, T. J., A. Grakoui, and C. M. Rice.** 1991. Processing of the yellow fever virus nonstructural polyprotein: a catalytically active NS3 proteinase domain and NS2B are required for cleavages at dibasic sites. J. Virol. **65:**6042–6050.

12. **Chambers, T. J., A. Nestorowicz, S. M. Amberg, and C. M. Rice.** 1993. Mutagenesis of the yellow fever virus NS2B protein: effects on proteolytic processing, NS2B-NS3 complex formation, and viral replication. J. Virol. **67:**6797–6807.

13. **Chu, P. W. G., and E. G. Westaway.** 1985. Replication strategy of Kunjin virus: evidence for recycling role of replicative form RNA as template in semiconservative and asymmetric replication. Virology **140:**68–79.

14. **Chu, P. W. G., and E. G. Westaway.** 1987. Characterization of Kunjin virus RNA-dependent RNA polymerase: reinitiation of synthesis in vitro. Virology **157:**330–337.

15. **Chu, P. W. G., and E. G. Westaway.** 1992. Molecular and ultrastructural analysis of heavy membrane fractions associated with the replication of Kunjin virus RNA. Arch. Virol. **125:**177–191.

16. **Chu, P. W. G., E. G. Westaway, and G. Coia.** 1992. Comparison of centrifugation methods for molecular and morphological analysis of membranes associated with RNA replication of the flavivirus Kunjin. J. Virol. Methods **37:**219–234.

17. **Coia, G., M. D. Parker, G. Speight, M. E. Byrne, and E. G. Westaway.** 1988. Nucleotide and complete amino acid sequences of Kunjin virus: definitive gene order and characteristics of the virus-specified proteins. J. Gen. Virol. **69:**1–21.

18. **Edward, Z., and T. Takegami.** 1993. Localization and functions of Japanese encephalitis virus nonstructural proteins NS3 and NS5 for viral RNA synthesis in the infected cells. Microbiol. Immunol. **37:**239–243.

19. **Egger, D., L. Pasamontes, R. Bolten, V. Boyko, and K. Bienz.** 1996. Reversible dissociation of the poliovirus replication complex: functions and interactions of its components in viral RNA synthesis. J. Virol. **70:**8675–8683.

20. **Falgout, B., M. Pethel, Y. M. Zhang, and C.-J. Lai.** 1991. Both nonstructural proteins NS2B and NS3 are required for the proteolytic processing of dengue virus nonstructural proteins. J. Virol. **65:**2467–2475.

21. **Falgout, B. F., R. H. Miller, and C.-J. Lai.** 1993. Deletion analysis of dengue virus type 4 nonstructural protein NS2B: identification of a domain required for NS2B-NS3 protease activity. J. Virol. **67:**2034–2042.

22. **Froshauer, S., J. Kartenbeck, and A. Helenius.** 1988. Alphavirus RNA replicase is located on the cytoplasmic surface of endosomes and lysomes. J. Cell Biol. **107:**2075–2086.

23. **Gould, E. A., A. Buckley, N. Cammack, A. D. T. Barrett, J. C. S. Clegg, R. Ishak, and M. G. R. Varma.** 1985. Examination of the immunological relationships between flaviviruses using yellow fever virus monoclonal antibodies. J. Gen. Virol. **66:**1369–1382.

24. **Grun, J. B., and M. A. Brinton.** 1987. Dissociation of NS5 from cell fractions containing West Nile virus-specific polymerase activity. J. Virol. **61:**3641–3644.

25. **Hobman, T. C., L. Woodward, and M. G. Farquhar.** 1992. The rubella virus E1 glycoprotein is arrested in a novel post-ER, pre-Golgi compartment. J. Cell. Biol. **118:**795–811.

26. **Hong, S. S., and M. L. Ng.** 1987. Involvement of microtubules in Kunjin virus replication. Brief report. Arch. Virol. **97:**115–121.

27. **Kapoor, M., L. Zhang, M. Ramachandra, J. Kusukawa, K. E. Ebner, and R. Padmanabhan.** 1995. Association between NS3 and NS5 proteins of dengue virus type 2 in the putative RNA replicase is linked to differential phosphorylation of NS5. J. Biol. Chem. **270:**19100–19106.

28. **Khromykh, A. A., H. Meka, and E. G. Westaway.** 1995. Preparation of recombinant baculovirus by transfection of a ligated cDNA fragment without prior plasmid amplification in E. coli. Biotechniques **18:**357–360.

29. **Khromykh, A. A., T. J. Harvey, M. Abedinia, and E. G. Westaway.** 1996. Expression and purification of the seven nonstructural proteins of the flavivirus Kunjin in the E. coli and the baculovirus expression systems. J. Virol. Methods **61:**47–58.

30. **Koonin, E. V.** 1993. Computer-assisted identification of a putative methyltransferase domain in NS5 protein of flaviviruses and lambda 2 protein of reovirus. J. Gen. Virol. **74:**733–740.

31. **Kuo, M.-D., C. Chin, S.-L. Hsu, J.-Y. Shiao, T.-M. Wang, and J.-H. Lin.** 1996. Characterization of the NTPase activity of Japanese encephalitis virus NS3 protein. J. Gen. Virol. **77:**2077–2084.

32. **Leary, K., and C. D. Blair.** 1980. Sequential events in the morphogenesis of Japanese encephalitis virus. J. Ultrastruct. Res. **72:**123–129.

33. **Lee, J.-Y., J. A. Marshall, and D. S. Bowden.** 1994. Characterization of rubella virus replication complexes using antibodies to double-stranded RNA. Virology **200:**307–312.

34. **Lin, C., S. M. Amberg, T. J. Chambers, and C. M. Rice.** 1993. Cleavage at a novel site in the NS4A region by the yellow fever virus NS2B-3 proteinase is a prerequisite for processing at the downstream 4A/4B signalase site. J. Virol. **67:**2327–2335.

35. **Mackenzie, J. M., M. K. Jones, and P. R. Young.** 1996. Immunolocalization of the dengue virus nonstructural glycoprotein NS1 suggests a role in viral RNA replication. Virology **220:**232–240.

36. **Mackenzie, J. M., M. K. Jones, and P. R. Young.** 1996. Improved membrane preservation of flavivirus-infected cells with cryosectioning. J. Virol. Methods **56:**67–75.

37. **Muylaert, I. R., T. J. Chambers, R. Galler, and C. M. Rice.** 1996. Mutagenesis of the N-linked glycosylation sites of the yellow fever virus NS1 protein: effects on virus replication and mouse neurovirulence. Virology **222:**159–168.

38. **Muylaert, I. R., R. Galler, and C. M. Rice.** 1997. Genetic analysis of the yellow fever virus NS1 protein: identification of a temperature-sensitive mutation which blocks RNA accumulation. J. Virol. **71:**291–298.

39. **Ng, M. L.** 1987. Ultrastructural studies of Kunjin-virus infected *Aedes albopictus* cells. J. Gen. Virol. **68:**577–582.

40. **Ng, M. L., and L. C. Corner.** 1989. Detection of some dengue-2 virus antigens in infected cells using immuno-microscopy. Arch. Virol. **104:**197–208.

41. **Ng, M. L., and S. S. Hong.** 1989. Flavivirus infection: essential ultrastructural changes and association of Kunjin virus NS3 protein with microtubules. Arch. Virol. **106:**103–120.

42. **Ng, M. L., J. S. Pedersen, B. H. Toh, and E. G. Westaway.** 1983. Immunofluorescent sites in Vero cells infected with the flavivirus Kunjin. Arch. Virol. **78:**177–190.

43. **Ng, M. L., W. K. P. Choo, and Y. L. Ho.** 1992. Detection of flavivirus antigens in purified infected cell membranes. J. Virol. Methods **39:**125–138.

44. **Ng, M. L., F. M. Yeong, and S. H. Tan.** 1994. Cryosubstitution technique reveals new morphology of flavivirus-induced structures. J. Virol. Methods **49:**305–314.

45. **Preugschat, F., C. W. Yao, and J. H. Strauss.** 1990. In vitro processing of dengue virus type 2 nonstructural proteins NS2A, NS2B, and NS3. J. Virol. **64:**4364–4374.

46. **Rice, C. M., E. M. Lenches, S. R. Eddy, S. J. Shin, R. L. Sheets, and J. H. Strauss.** 1985. Nucleotide sequence of yellow fever virus: implications for flavivirus gene expression and evolution. Science **229:**726–733.

47. **Speight, G., and E. G. Westaway.** 1989. Carboxy-terminal analysis of nine proteins specified by the flavivirus Kunjin: evidence that only the intracellular core protein is truncated. J. Gen. Virol. **70:**2209–2214.

48. **Speight, G., and E. G. Westaway.** 1989. Positive identification of NS4A, the last of the hypothetical nonstructural proteins of flaviviruses. Virology **170:**299–301.

49. **Speight, G., G. Coia, M. D. Parker, and E. G. Westaway.** 1988. Gene mapping and positive identification of the non-structural proteins NS2A, NS2B, NS3, NS4B and NS5 of the flavivirus Kunjin and their cleavage sites. J. Gen. Virol. **69:**23–34.

50. **Takegami, T., D. Sakamuro, and T. Furukawa.** 1994. Japanese encephalitis virus nonstructural protein NS3 has RNA binding and ATPase activities. Virus Genes **9:**105–112.

51. **Troxler, M., D. Egger, T. Pfister, and K. Bienz.** 1992. Intracellular localization of poliovirus RNA by *in situ* hybridization at the ultrastructural level using single-stranded riboprobes. Virology **191:**687–697.

52. **Warrener, P., J. K. Tamura, and M. S. Collett.** 1993. RNA-stimulated NTPase activity associated with yellow fever virus NS3 protein expressed in bacteria. J. Virol. **67:**989–996.

53. **Wengler, G., and G. Wengler.** 1991. The carboxy-terminal part of the NS3 protein of the West Nile flavivirus can be isolated as a soluble protein after proteolytic cleavage and represents an RNA-stimulated NTPase. Virology **184:**707–715.

54. **Wengler, G., and G. Wengler.** 1993. The NS3 nonstructural protein of flavivirus contains an RNA triphosphatase activity. Virology **197:**265–273.

55. **Wengler, G., T. Nowak, and E. Castle.** 1990. Description of a procedure which allows isolation of viral nonstructural proteins from BHK vertebrate cells infected with the West Nile flavivirus in a state which allows their direct chemical characterization. Virology **177:**795–801.

56. **Wengler, G., G. Czaya, P. M. Färber, and J. H. Hegemann.** 1991. *In vitro* synthesis of West Nile virus proteins indicates that the amino-terminal segment of the NS3 protein contains the active centre of the protease which cleaves the viral polyprotein after multiple basic amino acids. J. Gen. Virol. **72:**300–308.

57. **Westaway, E. G.** 1973. Proteins specified by group B togaviruses in mammalian cells during productive infections. Virology **51:**454–465.

58. **Westaway, E. G., and M. R. Goodman.** 1987. Variation in distribution of the three flavivirus-specified glycoproteins detected by immunofluorescence in infected Vero cells. Arch. Virol. **94:**215–228.

59. **Westaway, E. G., A. A. Khromykh, M. T. Kenney, J. M. Mackenzie, and M. K. Jones.** Proteins C and NS4B of the flavivirus Kunjin translocate independently into the nucleus. Virology, in press.

60. **Wubbolts, R., M. Fernandez-Borja, L. Oomen, D. Verwoerd, H. Janssen, J. Calafat, A. Tulp, S. Dusseljee, and J. Neefjes.** 1996. Direct vesicular transport of MHC class II molecules from lysosomal structures to the cell surface. J. Cell Biol. **135:**611–622.